Agrimoniin Sensitizes Pancreatic Cancer to Apoptosis through ROS-Mediated Energy Metabolism Dysfunction

Xiandong Zhu
Wenzhou Medical University First Affiliated Hospital: The First Affiliated Hospital of Wenzhou Medical University https://orcid.org/0000-0001-8106-2833

Feixiang Duan
Wenzhou Medical University First Affiliated Hospital: The First Affiliated Hospital of Wenzhou Medical University

Yongqiang Wang
Wenzhou Medical University First Affiliated Hospital: The First Affiliated Hospital of Wenzhou Medical University

Hewei Zhang
Wenzhou Medical University First Affiliated Hospital: The First Affiliated Hospital of Wenzhou Medical University

Xiaowu Wang
Wenzhou Medical University First Affiliated Hospital: The First Affiliated Hospital of Wenzhou Medical University

Yan Zhang
Wenzhou Medical University First Affiliated Hospital: The First Affiliated Hospital of Wenzhou Medical University

Hengjie Tang
Wenzhou Medical University First Affiliated Hospital: The First Affiliated Hospital of Wenzhou Medical University

Hongjian Huang
Wenzhou Medical University First Affiliated Hospital: The First Affiliated Hospital of Wenzhou Medical University

Bicheng Chen
Wenzhou Medical University First Affiliated Hospital: The First Affiliated Hospital of Wenzhou Medical University

Linxiao Sun (sunlinxiao@wmu.edu.cn)
Wenzhou Medical University First Affiliated Hospital: The First Affiliated Hospital of Wenzhou Medical University

Research

Keywords: Pancreatic cancer, Agrimoniin, ROS, Energy metabolism

Posted Date: April 6th, 2021

DOI: https://doi.org/10.21203/rs.3.rs-389385/v1

Version of Record: A version of this preprint was published at Phytomedicine on October 1st, 2021. See the published version at https://doi.org/10.1016/j.phymed.2021.153807.

Abstract

Background

Agrimoniin, a polyphenol compounds isolated from *Agrimonia pilosa ledeb*, has antiviral, antimicrobial, and anticancer activities in vivo and in vitro. However, its molecular mechanism in pancreatic cancer remains to be determined.

Methods

The proliferation was detected by colony formation, cell proliferation and toxicity, and real-time cell analysis techniques. The apoptosis was detected by flow cytometry and Western blot. Flow cytometry was used to measure the level of reactive oxygen species (ROS) and apoptosis. The level of intracellular ROS or mitochondrial membrane potential was measured with a DCFH-DA or JC-1 probe. Cell metabolism assays were analyzed and evaluated by using Agilent Seahorse Bioscience XF96 Extracellular Flux Analyzer. The target proteins were analyzed by Western blot. Subcutaneous cancer models in nude mice were established to evaluate the anticancer effects in vivo.

Results

Agrimoniin inhibited cell growth and promoted cell apoptosis by regulating cell metabolism in pancreatic cancer cells. Agrimoniin increased the ROS level in pancreatic cancer cells by suppressing Nrf2-dependent ROS scavenging system and disrupting normal mitochondrial membrane potential. We also found that agrimoniin significantly disrupted mitochondrial function and reduced the protein expression of mTOR/HIF-1α pathway and subsequently decreased oxygen consumption rate and extracellular acidification rate. Eventually, agrimoniin affected intracellular energy metabolism and induced apoptosis of pancreatic cancer cells.

Conclusions

These findings reveal the novel function of agrimoniin in promoting apoptosis of pancreatic cancer cells through mediating energy metabolism dysfunction.

Background

Pancreatic cancer is a highly malignant gastrointestinal tumor with a poor prognosis[1]. Many patients with pancreatic cancer are already in the middle or late stages when they are diagnosed and have a short five-year survival rate (approximately 10%) in the USA[2, 3]. Hence, chemotherapy has become the most common treatment for patients with late-stage pancreatic cancer who cannot undergo an operation[4].

However, in most cases, patients with pancreatic cancer respond poorly to chemotherapy or radiation therapy and may be accompanied by serious adverse reactions, such as liver toxicity, renal toxicity, gastrointestinal bleeding, and cardiovascular toxicity[5, 6]. Therefore, exploring new chemotherapy drugs to treat and prevent this fatal disease is imperative.

Studies have found a great difference between normal differentiated cells and cancer cells in metabolic requirements[7]. The mitochondrial oxidative phosphorylation process produces more than 90% of the energy for cellular processes for normally differentiated cells[8]. However, most malignant cells obtain energy through an increased rate of aerobic glycolysis rather than oxidative phosphorylation[9, 10]. However, the efficiency of glycolysis to produce adenosine triphosphate (ATP) in cancer cells is not as high as that of oxidative phosphorylation[11]. To acclimatize to the situation of infinite proliferation and metastasis, cancer cells must increase their glucose uptake to produce a large amount of energy[10]. This phenomenon, which is known as the Warburg effect, depends on aerobic glycolysis[12]. New studies have shown that inhibition of glycolysis will kill malignant cancer cells while have little or no effect on normal cells[12, 13]. Therefore, targeted glycolysis is a new method to regulate the hyperproliferation of cancer and a promising strategy for precision therapy of cancer.

Reactive oxygen species (ROS) generally referred to as “highly reactive oxygen free radicals” that are produced in cells through multiple mechanisms and regulate cell metabolism, proliferation, and apoptosis [14, 15]. ROS in cancer cells not only responds to external factors but is also produced endogenously by a byproduct of other biological reactions or as various physiological processes in cell itself[16, 17]. Although low and medium levels of ROS are beneficial to the growth of tumor cells, overaccumulation of ROS may lead to cell dysfunction and apoptosis[18]. For example, sophoridine increases the generation of ROS and induces cell apoptosis in pancreatic cancer cells[19]. Ciclopirox olamine provokes ROS levels and induce autophagy and mitochondrial-related apoptosis in rectal cancer cells [20]. Therefore, regulating the levels of ROS is important to affect the occurrence and development of cancer.

In recent years, Chinese herbal medicine natural products have attracted wide attention from medicinal chemists and clinicians due to their lower toxicity and rich structural diversity[21]. Agrimoniin, a polyphenol compounds isolated from *Agrimonia pilosa ledeb*[22], metabolized by human intestinal flora and has antiviral, antimicrobial, and other biological activities in vivo and in vitro[23–26]. Agrimoniin also has been reported to have a strong cytotoxic effect on gastric cancer cells (SGC-7901) and mouse mammary carcinoma (MM2) cells in vitro[26, 27]. Moreover, it can inhibit the growth of MM2 cancer, MH134 hepatoma, and fibrosarcoma solid-type tumors[26, 28].

However, the effect of agrimoniin in pancreatic cancer and its underlying mechanism have not been thoroughly explored and reported. Here, we demonstrate that agrimoniin has a strong anti-tumor effect and show that it can significantly increase intracellular ROS levels, interfere with mitochondria functions, and diminish glycolysis to cause cancer apoptosis.

Materials And Methods

Cell culture and reagents

Human pancreatic cancer cell lines PANC-1 and CFPAC-1 were obtained from the Cell Bank of the Chinese Academy of Sciences (Shanghai, China). The cells were maintained in DMEM medium (Invitrogen, CA, USA) (PANC-1) or RPMI-1640 (Invitrogen, CA, USA) (CFPAC-1) containing 10% FBS (Gibco, NY, USA) and 100 U/mL penicillin-streptomycin (Invitrogen, CA, USA). All cell lines were maintained at 37 °C and 5% CO_2. Agrimoniin was provided by YuanYe Biotechnology (Shanghai, China). N-acetylcysteine (NAC) and MHY1485 were purchased from MedChemExpress (MCE, Shanghai, China) and used to pretreat the cancer cells for 1 h before agrimoniin treated (0 or 300 μmol/L).

Cell viability assay

The cells were plated and cultured for 24 h in 96-well plates with 5.0×10^3 cells/well. After being grown overnight, the cells were cultured another 24 h with different drug concentrations. Then, CCK-8 (Cell Counting Kit-8, Dojindo, Shanghai, China) reagent (10 μl) was incubated with each pore for 1 h. The absorbance of the dissolved solutions was determined at 450 nm (Thermo Scientific Varioskan FlashUSA).

Real-time cellular analysis

In this study, about 2×10^5 cells/well were seeded in cell culture E16 plates and cultured for 24 h. During the whole experiment, the effects of different drug concentrations on cell proliferation were automatically monitored every 15 minutes by using the xCELLigence MP system (ACEA Biosciences, San Diego, California, USA).

Colony formation assay

The cancer cells were evenly inoculated in 6-well plates with 1000–2000 cells per well. After the cells formed cell colonies in the incubator for one week, the corresponding concentrations of drugs were added and cultured for another 24 h. Then, the number of clones was counted after fixing and staining.

Cell apoptosis analysis

The cells were cultured in a 6-well plate to a certain number, then incubated for another 24 h after drug treatment. Next, the adherent and suspension cells were collected and the resuspended cells were incubated with 5 μL Annexin V-FITC (BD Biosciences, San Jose, CA, USA) for 15 min and 5 μL propidium iodide (PI) (BD Biosciences, San Jose, CA, USA) for 5 min in the dark at room temperature. Apoptosis of cultured cells was performed using flow cytometry (BD FACSVerse™, BD Biosciences, San Jose, CA, USA).

Western blot assay

Total proteins were separated from cultured cells and analyzed by Western blotting as performed as previously reported protocols[29]. The membranes were probed with specific primary antibodies against Bcl2 (CST, #3498, 1:1000), Bax (CST, #2772, 1:1000), PI3K (CST, #4257, 1:1000), AKT (CST, #4691, 1:1000), p-mTOR (CST, #5536, 1:1000), mTOR (Abcam, ab87540, 1:1000), cleaved caspase-3 (Abcam, ab2302,1:1000), Ki67 (Affinity Biosciences, AF0198, 1:1000), Nrf2 (Affinity Biosciences, AF0639, 1:1000), HO-1 (Affinity Biosciences, AF5393, 1:1000), p-PI3K (Affinity Biosciences, AF3242, 1:1000), p-AKT (Affinity Biosciences, AF0016, 1:1000), HIF-1α (Affinity Biosciences, AF1009, 1:1000), LDHA (Affinity Biosciences, DF6280, 1:1000), and β-actin (Proteintech, 66009–1-Ig, 1:2000) overnight at 4 °C. The addition of ECL substrate (Thermo Fisher Scientific) was used for visualization. Lastly, the protein membranes were analyzed using Image-Pro Plus software (version 6.0) and normalized with β-actin protein levels.

Tumor xenograft assay

Male nude mice (BALB/c), six-week-old, were purchased from Weitong Lihua Experimental Animal Technology (Beijing, China) and placed in SPF-level conditions. Resuspended CFPAC-1cells (1×10^6 in 100 μL PBS) were subcutaneously inoculated in the side of right flank of the nude mice. After tumors were visible, the mice were randomly divided into two groups (n = 4/group): control (100 μL of PBS) and Agrimoniin (20 mg/kg). All mice were treated with intraperitoneal injection once a daily. Tumor size was measured and calculated by the formula V = π/6 × larger length × width^2 every 5 days for 30 days. All animals were sacrificed after 30 days. The xenografted tumor weights were measured and fixed in 4% paraformaldehyde solution or Tissue-Tek O.C.T. Compound (SAKURA; USA).

Histopathological examination and immunohistochemical staining

Hematoxylin-eosin (HE) staining and immunohistochemical staining of tumor sections were performed as previously reported protocols[30]. Primary antibodies added to the sections were p-mTOR (CST, #5536, 1:200), Nrf2 (Affinity Biosciences, AF0639, 1:200). The images were taken using a microscope (Olympus, Tokyo, Japan) and analyzed with Image-Pro Plus 6 software.

Immunofluorescence assay

The four-micron frozen tumor sections were fixed with 4% formaldehyde for 30 min and then permeabilized with 0.1% Triton X-100 (Beyotime, Shanghai, China) at room temperature for 10 min. After being washed with PBS three times, the cells were blocked with 5% bovine serum albumin (BSA) at room temperature for another 30 min. The primary antibody cleaved caspase-3 (Abcam, ab2302,1:200), Ki67 (Affinity Biosciences, AF0198, 1:200), and HIF-1α (Affinity Biosciences, AF1009, 1:1000) were incubated overnight at 4 °C. After washing, the Cora Lite 488 conjugated goat anti-rabbit secondary antibodies (1:400) were added to the cells for 1 h at 37 °C. Lastly, the nuclei of the cells were stained with DAPI (Solarbio, C0065, Peking, China) and observed using a confocal microscope (Leica, Germany) or fluorescence microscope (Olympus, Tokyo, Japan).

TUNEL assays

TUNEL staining was utilized to evaluate the apoptosis in tumor tissues by using the In Situ Cell Death Detection Kit (Roche). The fixed tumor slides (4 μm) were incubated with proteinase-K (20 mg/mL) for 15 min at 37 °C. After being washed with PBS, the sections were incubated with TUNEL reaction mixture (50 μL) for 1 h at 37 °C. The nuclei of the cells were stained with DAPI (Solarbio, C0065, Peking, China) and observed using a fluorescence microscope (Olympus, Tokyo, Japan).

Quantitative reverse transcriptase-PCR (qRT-PCR)

Total RNA was isolated from pancreatic cancer cells using a TRIzol Kit (Invitrogen, USA). Each sample was subjected to reverse transcription by using the RevertAid First Strand cDNA Synthesis Kit (Thermo Fisher Scientific, MA, USA). The mRNA expression levels were measured with the SYBR-Green Master Mix kit (Roche, IN, USA) by using a PCR detection system (Bio-Rad CFX96, USA). The specific sequences of the primers were as follows: β-Actin forward: AGAAAATCTGGCACCACACC, reverse: AGAGGCGTACAGGGATAGCA; HO-1 forward: ATTCTCTTGGCTGGCTTC, reverse: CTGGATGTGCTTTTCGTT; NQO1 forward: CATCCCAACTGACAACCA, reverse: GAAGCCTGGAAAGATACCC.

ROS assay

The intracellular levels of ROS were detected by 2,7-dichlorofluorescin-diacetate (DCFH-DA) (Nanjing Jiancheng Bioengineering Institute, Nanjing, China). After being treated with drugs the cells were incubated with 10 μM DCFH-DA at 37 °C for 30 min in the dark. The dye was then removed by PBS and the cells were immediately observed under a fluorescence microscope (Nikon Corporation, Tokyo, Japan). For flow cytometry, according to the above method, the washed cells were resuspended in PBS, and fluorescence was detected by using the flow cytometer (BD FACSVerse™, BD Biosciences, San Jose, CA, USA). For tissues, the four-micron frozen tumor sections were incubated with DCFH-DA for 30 min at 37 °C in the dark. The ROS level of tissues was measured by a fluorescence microscope (Olympus, Tokyo, Japan).

Mitochondrial membrane potential (ΔΨm) assay

Changes in the mitochondrial membrane potential of the treated cells were measured by using a mitochondrial membrane potential assay kit (Beyotime Co. China). We added enough JC-1 (fluorescent probe) working solution to the plates to cover all cells for 30 min at 37 °C. Then, the cells were observed under a fluorescence microscope (Nikon Corporation, Tokyo, Japan). Fluorescence changes from red (high ΔΨm) to green (low ΔΨm) may indicate mitochondrial dysfunction.

Cell metabolism assays

The intact cellular oxygen consumption rate (OCR) was measured by the Mito Stress Test Kit (Agilent, 03015–100, USA), and the extracellular acidification rate (ECAR) was measured by the Glycolytic Stress Test Kit (Agilent, 103020–100, USA) and detected in the Seahorse XF96 Extracellular Flux Analyzer (Seahorse Bioscience, North Billerica, MA, USA). The cells were seeded into XF96 cell culture microplates (Seahorse Bioscience) and allowed to incubate overnight at 37 °C. After being pretreated with different

concentrations, the cells were incubated for another 24 h. Simultaneously, the calibration plates (with calibration solution) and the assay solution (for OCR: oligomycin, 2.5 μM; FCCP, 2 μM; rotenone, 0.25 μM; and anti-mildew A,0.25 μM, and for ECAR: glucose, 10 mM, oligomycin, 1 μM; and 2-DG, 50 mM) were incubated overnight in a 37 °C CO_2-free incubator. Before metabolism measurement, both cell culture media were replaced with the assay solution. Lastly, the cell plate was replaced with a probe plate after the probe calibration was completed.

Statistical analysis

Data were stated as mean ± standard error of the mean (SEM). All data were statistically analyzed by using GraphPad Prism 7 software (GraphPad Software, Inc., La Jolla, CA, USA). The significance of differences was analyzed by the Student's t-test for unpaired data or one-way analysis of variance, preceded by Dunnett's multiple comparison test where appropriate. P-values <0.05 were considered statistically significant. Each experiment was repeated at least three times.

Results

Agrimoniin inhibits the proliferation and induces the apoptosis of pancreatic cancer cells

CCK-8 assay, RTCA, and colony formation assay were performed to investigate the inhibitory activity of agrimoniin in tumor growth. The chemical structure of agrimoniin is shown in Fig. 1a. As shown in Fig. 1b, the half-maximal inhibitory concentration (IC50) values of agrimoniin on PANC-1 and CFPAC-1 pancreatic cancer cells for 24 h were 269.4 and 296.8 μM, respectively. Therefore, agrimoniin of 100, 200, and 300 μM was selected for further study. As expected, the growth of PANC-1 and CFPAC-1 cells was significantly inhibited in a dose-dependent manner by agrimoniin treatment (100, 200, and 300 μM); RTCA and colony formation assay are shown in Fig. 1c–e. In the colony formation assay, the formed clones were assessed by crystal violet staining and counted manually for each group of cells. To confirm the effects of agrimoniin on apoptosis, we assessed the apoptosis of cells by flow cytometry analysis. The results show that the proportion of apoptosis and necrotic cells significantly increased with agrimoniin treatment (Fig. 1f–g). Western blot results showed that after agrimoniin treatment, the protein expression of Bax and cleaved caspase-3 in pancreatic cancer cells increased significantly, while the protein expression of Bcl-2 decreased significantly (Fig. 1h–i).

Agrimoniin inhibits tumor growth in vivo

To evaluate whether a similar inhibitory effect of agrimoniin on pancreatic cancer growth in vivo exists, we conducted an experiment that involves intraperitoneal injection of agrimoniin (20 mg/kg/day) or an equal volume of PBS for 25 consecutive days to mice of the nude mouse xenograft model. As shown in Fig. 2a–c, the volume and weight of tumors were significantly reduced under agrimoniin treatment. HE staining showed a relatively higher density of necrotic cells and a low density of tumor cells after agrimoniin treatment in xenograft tumor sections (Fig. 2d). Immunofluorescence assay of xenograft tumor tissues indicated that agrimoniin treatment significantly repressed the expression of Ki-67 (marker

of proliferation) (Fig. 2e) and increased the expression of cleaved caspase-3 (marker of apoptosis) (Fig. 2f). Similarly, TUNEL analysis demonstrated that the rate of apoptosis cells in agrimoniin-treated tumors increased significantly (Fig. 2g). Thus, agrimoniin inhibited growth and induced apoptosis in vivo.

Agrimoniin treatment increases the ROS production in PANC-1 and CFPAC-1 cells

To evaluate the effect of agrimoniin treatment on the ROS level in pancreatic cancer cells, several methods of vivo and in vitro detection were used. First, the ROS levels in cancer cells were investigated using flow cytometry analysis. Figs. 3a and 3b show an accumulation of ROS in cells after exposure to indicated concentrations of agrimoniin for 24 h and that it increased in a dose-dependent manner. Second, DCFH-DA was adopted to detect ROS levels, and we demonstrated that agrimoniin treatment significantly increased the DCF fluorescence intensity by using fluorescence microscopy in cells (Fig. 3c). Similarly, the xenograft tumor tissues derived from the agrimoniin-treated group exhibited higher ROS accumulation (Fig. 3d). To further explore the source of excessive ROS production by agrimoniin, we detected the changes in antioxidant response signals and mitochondrial membrane potential. We found that agrimoniin inhibits the protein levels of Nrf2 and HO-1 via Western blot analysis (Fig. 3e, f). Furthermore, agrimoniin markedly downregulated the transcription levels of Nrf2 target genes (HO-1 and NQO1) via qRT-PCR analyses (Fig. 3g). Similarly, we identified proteasomal downregulated expression of Nrf2 (Fig. 3h) and repressed expression of HO-1 in xenograft tumor sections (Fig. 3i). Consistent with the increased ROS production, the ΔΨm was significantly decreased after treatment with agrimoniin (0, 100, 200, and 300 μM) for 24 h (Fig. 4a, b). Altogether, these observations suggest that ROS production was increased after agrimoniin-treated in pancreatic cancer cells.

Agrimoniin induces metabolic reprogramming in pancreatic cancer cells

In this study, we considered agrimoniin actions on energy metabolism and mitochondrial function. Similar to the above result, the ΔΨm was significantly decreased after agrimoniin treated for 24 h (Fig. 4a, b), while the mitochondrial respiration was significantly suppressed. In other words, agrimoniin dampened mitochondrial function, and the results of OCR (an indicator of mitochondrial oxidative phosphorylation [OXPHOS]) indicated that agrimoniin led to significant downregulation of basal respiration, maximal respiration, and ATP production in pancreatic cancer cells (Fig. 4c–f).

In addition, the protein expression of PI3K/AKT/mTOR pathway and the key genes it regulates (HIF-1α, LDHA) were significantly reduced after agrimoniin treatment (Fig. 5a, b). Specifically, in the drug-treated group in cancer cells (100, 200, and 300 μM)the protein levels of p-PI3K, p-Akt and p-mTOR were decreased significantly. With its essential role in metabolic reprogramming of cancer cells, HIF-1α and its target genes in agrimoniin-treated group were also reduced, which regulated the Warburg effect at the same time. Next, we analyzed the aerobic glycolytic rate in cancer cells with agrimoniin treatment. The results of ECAR (an indicator of cell glycolysis) showed that agrimoniin-treated cells significantly suppressed basal glycolysis, maximal glycolysis, and glycolytic capacity in cancer cells (100, 200, and 300 μM) (Fig. 5c–f). A similar tendency of p-mTOR was exhibited in agrimoniin-treated xenografts by IHC staining (Fig. 5g). Immunofluorescence analysis also showed that the HIF-1α-positive area of the

agrimoniin-treated xenograft samples was significantly reduced compared with the normal samples (Fig. 5h).

Overall, these data suggest that cancer treated with agrimoniin resulted in a significant reduction in energy metabolism. Interestingly, agrimoniin inhibited mitochondrial function and glycolysis, which might greatly enhance the inhibitory effect of the drug on cancer.

ROS is required for agrimoniin-induced metabolic reprogramming

To further confirm whether the accumulation of ROS was caused by an intrinsic link between agrimoniin and the changes in biological function in pancreatic cancer cells, we used an ROS inhibitor N-acetylcysteine (NAC) (Fig. 6a). The inhibitory effect of cell viability and the promotional effect of cell apoptosis caused by agrimoniin (300 μM) in pancreatic cancer cells were abolished after pretreatment with NAC (5 mM) (Fig. 6b–d). JC-1 assays showed that the change of ΔΨm was significantly reversed after pretreatment with NAC (Fig. 6e, f), while the mitochondrial function was similarly reversed (Fig. 6g), as indicated by reduced levels of basal respiration, maximal respiration, and ATP production (Fig. 6h). In addition, pretreatment with NAC reversed the change in protein expression of p-PI3K, p-AKT, and p-mTOR via Western blot assays (Fig. 6i, g). Similar results were obtained in ECAR, and the basal glycolysis, maximal glycolysis, and glycolytic capacity in pancreatic cancer cells were increased by NAC pretreatment despite agrimoniin treatment (Fig. 6k, l). Collectively, these findings reveal that agrimoniin induces mitochondrial dysfunction and metabolic reprogramming through accumulation of cellular ROS in pancreatic cancer cells, thereby promoting cell apoptosis.

Enhancing mTOR/HIF-1α signaling abolishes the effects of agrimoniin on glycolysis

To evaluate whether agrimoniin regulated the cell metabolism of cancer cells by mediating the mTOR/HIF-1α pathway, we performed a rescue experiment by pretreatment with MHY1485 (mTOR activity). Pretreatment with MHY1485 (15 μM) increased protein expression of p-mTOR, HIF-1α and LDHA in cancer cells despite agrimoniin treatment (300 μM). Enhancing mTOR/HIF-1α signaling abolished the inhibitory effect of agrimoniin on cancer cell viability (Fig. 7c) and the promotional effect of cell apoptosis (Fig. 7d, e). Importantly, mTOR activator counteracted the decreased glycolysis induced by agrimoniin (Fig. 7f). Consistent with the above result, the basal glycolysis, maximal glycolysis, and glycolytic capacity in pancreatic cancer cells were increased by MHY1485 pretreatment (Fig. 7g). These data suggest that agrimoniin inhibits glycolysis and induces cell apoptosis through the mTOR/HIF-1α signaling in pancreatic cancer cells.

Discussion

In clinical cancer treatment, although conventional chemotherapy is the main method of human cancer treatment, its low response rates, severe toxicities, and drug resistance will greatly reduce the quality of life of patients[31]. Hence, identifying new drug targets and finding an effective and safe drug to better treat pancreatic cancer are urgently needed. In this study, we demonstrated that agrimoniin has a strong

anti-tumor effect in vitro and in vivo. Moreover, the mechanism of agrimoniin treatment via regulating intracellular ROS levels may induce mitochondrial dysregulation and mediate PI3K/Akt/mTOR pathway to affect intracellular energy metabolism, thereby inducing pancreatic cancer apoptosis.

ROS are highly reactive molecules that are produced from both endogenous and exogenous sources[32]. The formation of ROS in mammalian cells can be caused by mitochondria, peroxisomes, endoplasmic, plasma membranes, and NADPH oxidase as endogenous sources or by UV or ionizing radiation as exogenous sources[19, 33]. Increased production of ROS has been detected in multiple cancer cells and has been shown to have a variety of effects[34, 35]. For example, they can activate protumor signals, enhance cell survival and proliferation, and drive DNA damage and genetic instability[36]. However, ROS can also promote the generation of antitumor signals and initiate tumor cell death induced by oxidative stress[37, 38]. Nrf2 is a main transcription factor of antioxidant defense modules that can regulate oxidative and stress injury[39]. Changes in the Nrf2 level will affect the intracellular ROS level, which in turn affects the occurrence and development of cancer[40]. According to the different redox balance between cancer cells and normal differentiated cells, affecting the ROS levels in cancer cells may be a potential strategy for cancer therapy. In this study, we showed that agrimoniin treatment could effectively inhibit the proliferation and promote apoptosis of PANC-1 and CFPAC-1 pancreatic tumor cells. At the same time, the expression of Nrf2, HO-1 (antioxidant enzymes) decreased, whereas the production of ROS increased. The results indicate that agrimoniin affects the level of cellular ROS and promotes apoptosis in pancreatic cancer cells.

Mitochondria are essential organelles for oxidative phosphorylation generation[41] and are one of the main sources of endogenous ROS. Under normal circumstances, the increase in the production of ROS leads to a compensatory increase in antioxidant levels, which may protect mitochondria and other organelles[42]. With excessive production of ROS and/or depletion of antioxidants, ROS balance will be disrupted and cause oxidative stress[37]. Interestingly, mitochondria are also the main targets of ROS damage, which in turn destroys the function of mitochondria and leads to excessive ROS generation[43–45]. Excessive oxidative stress can lead to the collapse of ΔΨm and mitochondrial membrane structure[46, 47]. The integrity of the mitochondrial membrane serves important roles in the mitochondrial OXPHOS process, which is mainly responsible for the production of ATP in the cell[48]. In this study, pancreatic cancer cells treated with agrimoniin disrupt mitochondrial function and significantly decrease mitochondrial membrane potential, as reflected by a decrease in OCR (an indicator of mitochondrial OXPHOS)[49] and ATP production. The collapse of mitochondria function can reduce the energy supply of cancer cells, affect the growth of cancer cells, and promote the death of cells. Importantly, NAC, a ROS scavenger, inhibited the significant increase the production of ROS with agrimoniin treatment. Moreover, NAC abolished the inhibitory effect of agrimoniin on OCR and ATP levels, restored the mitochondrial transmembrane potential, and ultimately reduced cell apoptosis in pancreatic cancer. Taken together, agrimoniin promotes the cell apoptosis in pancreatic cancer, which may be related to ROS-mediated mitochondrial damage.

Cancer metabolism has a peculiar feature called the Warburg effect, which relies on aerobic glycolysis rather than the mitochondrial OXPHOS system to produce ATP, provide energy, and ensure cell survival[50]. As aforementioned, targeting the different metabolism between cancer cells and normal cells is an attractive therapeutic target for cancer treatment. HIF-1α plays an critical role in reprogramming cancer metabolism and regulating glycolytic enzymes because of the Warburg effect in cancerous cells [51, 52]. HIF-1α regulates glycolysis pathway, such as HK1, GLUT-1, and LDHA[53–55]. Among them, LDHA is a master regulator in glycolysis metabolism and can promote glycolysis by converting pyruvate into lactic acid and maintain cancer growth[53]. The PI3K signaling regulates many cellular processes, such as cell growth, proliferation, metabolism, and cancer progression[56]. Previous studies found that the mammalian target of PI3K/Akt/mTOR regulates glycolysis by affecting HIF-1α and other pathways[43]. Consistent with these results, agrimoniin reduced the protein levels of HIF-1α and LDHA by regulating the PI3K/AKT/mTOR activation. In addition, by detecting the ECAR[57], we found that the glycolysis ability of pancreatic cancer cells was inhibited significantly with agrimoniin treatment and promoted the further death of cells by reducing the energy supply considerably. Through the use of the mTOR activator (MHY1485), the experimental results further confirm that PI3K/Akt/mTOR signaling is a critical mediator of the effect of agrimoniin on glycolysis.

Conclusions

In summary, this study reveals the novel function of agrimoniin in inhibiting the proliferation of pancreatic cancer and promoting cell apoptosis through ROS-mediated energy metabolism dysfunction in pancreatic cancer cells. Interestingly, unlike other drugs, agrimoniin showed a dual inhibitory effect on ATP production. In detail, agrimoniin may regulate the production of intracellular ROS, damage the mitochondrial membrane potential and its function, mediate the inhibition of the PI3K/Akt/mTOR signaling pathway, and affect intracellular energy metabolism, thereby inducing apoptosis of pancreatic cancer cells. This research suggests that agrimoniin may become a potential drug in the treatment of pancreatic cancer. However, the anti-tumor mechanisms of probable binding position and interaction mode of the molecules of agrimoniin remain unclear and need to be explored in our next work. Altogether, the potential new targets and their synergies discovered in this research are of great significance for cancer treatment and drug development.

Abbreviations

DCFH-DA: 2,7-dichlorofluorescin-diacetate; ROS: reactive oxygen species; OCR: oxygen consumption rate; ECAR: extracellular acidification rate; ATP:adenosine triphosphate; ΔΨm: Mitochondrial membrane potential; NAC: N-acetylcysteine; OXPHOS: mitochondrial oxidative phosphorylation; Nrf2: NF-E2-related factor 2; HO-1: Heme oxygenase-1; NQO1: NAD(P)H: quinone oxidoreductase 1; PI3K: Phosphatidylinositol-3- kinase; mTOR: Mammalian target of rapamycin; HIF-1α: Hypoxia-inducible factor-1α; LDHA: Lactate dehydrogenase A

Declarations

Acknowledgements

The authors sincerely thank Hengjie Tang for his suggestions for this study.

Authors' contributions

ZXD did most of experiments and wrote the original draft. DFX took part in cell culture and helped revise the manuscript. WYQ took part in study in vivo. WXW took part in western blot assay. ZY and ZHW carried out the experiments and performed statistical analysis. THJ and HHJ provided valuable suggestions and helped revise the manuscript. CBC and SLX led study design and optimize experimental protocols. All authors read and approved the final manuscript.

Funding

This work was supported by the Wenzhou Municipal Science and Technology Bureau grant (Y20190073), Natural Science Foundation of Zhejiang Province (LQ20H030004).

Availability of data and materials

All data generated or analyzed during this study are included in this published article.

Ethics approval and consent to participate

All strategies were followed the Institutional Review Board of the Laboratory Animal Management Committee of Zhejiang Province and complies with the Guide for the Care and Use of Laboratory Animals (NIH Publication No. 85–23, revised 1996). All animal experiments were approved by the Institutional Animal Committee of Wenzhou Medical University for medical laboratory animal sciences (ID Number wydw2017-0008).

Consent for publication

Not applicable.

Competing interests

The authors declare that they have no competing interests.

Author details

1. Key Laboratory of Diagnosis and Treatment of Severe Hepato-Pancreatic Diseases of Zhejiang Province, The First Affiliated Hospital of Wenzhou Medical University, Wenzhou, 325000 Zhejiang Province, China

References

1. Hao L, Liu L, Meng X, Yu G, Li E, and Gu H: Evaluation of different b-values in DWI and 1H MRS for pancreatic cancer and pancreatitis: a rabbit model. Bioscience reports 2019; 39.
2. Wang R, Lai Q, Tang L, Tao Y, Yao Y, Liu Y, et al.: A novel 5T4-targeting antibody-drug conjugate H6-DM4 exhibits potent therapeutic efficacy in gastrointestinal tumor xenograft models. American journal of cancer research 2018; 8: 610-623.
3. Mizrahi J, Surana R, Valle J, and Shroff R: Pancreatic cancer. Lancet (London, England) 2020; 395: 2008-2020.
4. Zhao J, Schlößer H, Wang Z, Qin J, Li J, Popp F, et al.: Tumor-Derived Extracellular Vesicles Inhibit Natural Killer Cell Function in Pancreatic Cancer. Cancers 2019; 11.
5. Yao W, Maitra A, and Ying H: Recent insights into the biology of pancreatic cancer. EBioMedicine 2020; 53: 102655.
6. de Sousa Cavalcante L and Monteiro G: Gemcitabine: metabolism and molecular mechanisms of action, sensitivity and chemoresistance in pancreatic cancer. European journal of pharmacology 2014; 741: 8-16.
7. Soumoy L, Schepkens C, Krayem M, Najem A, Tagliatti V, Ghanem G, et al.: Metabolic Reprogramming in Metastatic Melanoma with Acquired Resistance to Targeted Therapies: Integrative Metabolomic and Proteomic Analysis. Cancers 2020; 12.
8. Yang Y, Cimen H, Han M, Shi T, Deng J, Koc H, et al.: NAD+-dependent deacetylase SIRT3 regulates mitochondrial protein synthesis by deacetylation of the ribosomal protein MRPL10. The Journal of biological chemistry 2010; 285: 7417-29.
9. Vander Heiden M, Cantley L, and Thompson C: Understanding the Warburg effect: the metabolic requirements of cell proliferation. Science (New York, N.Y.) 2009; 324: 1029-33.
10. Yin C, Lu W, Ma M, Yang Q, He W, Hu Y, et al.: Efficacy and mechanism of combination of oxaliplatin with PKM2 knockdown in colorectal cancer. Oncology letters 2020; 20: 312.
11. Zhou Y, Huang Y, Hu K, Zhang Z, Yang J, and Wang Z: HIF1A activates the transcription of lncRNA RAET1K to modulate hypoxia-induced glycolysis in hepatocellular carcinoma cells via miR-100-5p. Cell death & disease 2020; 11: 176.
12. Li W and Wang J: Uncovering the Underlying Mechanisms of Cancer Metabolism through the Landscapes and Probability Flux Quantifications. iScience 2020; 23: 101002.
13. Hong X, Zhong L, Xie Y, Zheng K, Pang J, Li Y, et al.: viaMatrine Reverses the Warburg Effect and Suppresses Colon Cancer Cell Growth Negatively Regulating HIF-1α. Frontiers in pharmacology 2019; 10: 1437.
14. Moreira H, Szyjka A, Paliszkiewicz K, and Barg E: Prooxidative Activity of Celastrol Induces Apoptosis, DNA Damage, and Cell Cycle Arrest in Drug-Resistant Human Colon Cancer Cells. Oxidative medicine and cellular longevity 2019; 2019: 6793957.

15. Kalil S, Rosa R, Capelli-Peixoto J, Pohl P, Oliveira P, Fogaça A, et al.: Immune-related redox metabolism of embryonic cells of the tick Rhipicephalus microplus (BME26) in response to infection with Anaplasma marginale. Parasites & vectors 2017; 10: 613.
16. Rejc B, Kato Y, Karas-Kuzelicki N, Osredkar J, and Gersak K: Lipid-lysine adducts and modified tyrosines as markers of oxidative stress in the second trimester of pregnancy and their association with infant characteristics. Experimental and therapeutic medicine 2016; 11: 797-805.
17. Cui J, Zhou Z, Yang H, Jiao F, Li N, Gao Y, et al.: MST1 Suppresses Pancreatic Cancer Progression via ROS-Induced Pyroptosis. Molecular cancer research : MCR 2019; 17: 1316-1325.
18. Starkov A: The role of mitochondria in reactive oxygen species metabolism and signaling. Annals of the New York Academy of Sciences 2008; 1147: 37-52.
19. Xu Z, Zhang F, Bai C, Yao C, Zhong H, Zou C, et al.: Sophoridine induces apoptosis and S phase arrest via ROS-dependent JNK and ERK activation in human pancreatic cancer cells. Journal of experimental & clinical cancer research : CR 2017; 36: 124.
20. Zhou J, Zhang L, Wang M, Zhou L, Feng X, Yu L, et al.: CPX Targeting DJ-1 Triggers ROS-induced Cell Death and Protective Autophagy in Colorectal Cancer. Theranostics 2019; 9: 5577-5594.
21. Sikander M, Malik S, Khan S, Kumari S, Chauhan N, Khan P, et al.: Novel Mechanistic Insight into the Anticancer Activity of Cucurbitacin D against Pancreatic Cancer (Cuc D Attenuates Pancreatic Cancer). Cells 2019; 9.
22. Grochowski D, Skalicka-Woźniak K, Orhan I, Xiao J, Locatelli M, Piwowarski J, et al.: A comprehensive review of agrimoniin. Annals of the New York Academy of Sciences 2017; 1401: 166-180.
23. Funatogawa K, Hayashi S, Shimomura H, Yoshida T, Hatano T, Ito H, et al.: Antibacterial activity of hydrolyzable tannins derived from medicinal plants against Helicobacter pylori. Microbiology and immunology 2004; 48: 251-61.
24. Koshiura R, Miyamoto K, Ikeya Y, and Taguchi H: Antitumor activity of methanol extract from roots of Agrimonia pilosa Ledeb. Japanese journal of pharmacology 1985; 38: 9-16.
25. Murayama T, Kishi N, Koshiura R, Takagi K, Furukawa T, and Miyamoto K: Agrimoniin, an antitumor tannin of Agrimonia pilosa Ledeb., induces interleukin-1. Anticancer research 1992; 12: 1471-4.
26. Miyamoto K, Kishi N, and Koshiura R: Antitumor effect of agrimoniin, a tannin of Agrimonia pilosa Ledeb., on transplantable rodent tumors. Japanese journal of pharmacology 1987; 43: 187-95.
27. Miyamoto K, Murayama T, Hatano T, Yoshida T, and Okuda T: Host-mediated anticancer activities of tannins. Basic life sciences 1999; 66: 643-63.
28. Miyamoto K, Kishi N, Koshiura R, Yoshida T, Hatano T, and Okuda T: Relationship between the structures and the antitumor activities of tannins. Chemical & pharmaceutical bulletin 1987; 35: 814-22.
29. Sun L, Zhu X, Luo J, Wang C, and Chen B: Role of DNA damage in the progress of chronic tubule-interstitial injury. Molecular medicine reports 2020; 22: 1081-1089.

30. Zhu X, Guo F, Tang H, Huang C, Xie G, Huang T, et al.: κIslet Transplantation Attenuating Testicular Injury in Type 1 Diabetic Rats Is Associated with Suppression of Oxidative Stress and Inflammation via Nrf-2/HO-1 and NF-B Pathways. Journal of diabetes research 2019; 2019: 8712492.
31. Reddy T, Garikapati K, Reddy S, Reddy B, Yadav J, Bhadra U, et al.: Simultaneous delivery of Paclitaxel and Bcl-2 siRNA via pH-Sensitive liposomal nanocarrier for the synergistic treatment of melanoma. Scientific reports 2016; 6: 35223.
32. Phaniendra A, Jestadi D, and Periyasamy L: Free radicals: properties, sources, targets, and their implication in various diseases. Indian journal of clinical biochemistry : IJCB 2015; 30: 11-26.
33. Ullah R, Khan M, Shah S, Saeed K, and Kim M: Natural Antioxidant Anthocyanins-A Hidden Therapeutic Candidate in Metabolic Disorders with Major Focus in Neurodegeneration. Nutrients 2019; 11.
34. Barr P, Miller T, Friedberg J, Peterson D, Baran A, Herr M, et al.: Phase 2 study of imexon, a prooxidant molecule, in relapsed and refractory B-cell non-Hodgkin lymphoma. Blood 2014; 124: 1259-65.
35. Arthikala M, Montiel J, Sánchez-López R, Nava N, Cárdenas L, and Quinto C: RhizobiumRespiratory Burst Oxidase Homolog Gene A Is Crucial for Infection and Nodule Maturation and Function in Common Bean. Frontiers in plant science 2017; 8: 2003.
36. Moloney J and Cotter T: ROS signalling in the biology of cancer. Seminars in cell & developmental biology 2018; 80: 50-64.
37. Kondo N, Nakamura H, Masutani H, and Yodoi J: Redox regulation of human thioredoxin network. Antioxidants & redox signaling 2006; 8: 1881-90.
38. Nogueira V, Park Y, Chen C, Xu P, Chen M, Tonic I, et al.: Akt determines replicative senescence and oxidative or oncogenic premature senescence and sensitizes cells to oxidative apoptosis. Cancer cell 2008; 14: 458-70.
39. Yu X, Chi X, Wu S, Jin Y, Yao H, Wang Y, et al.: Dexmedetomidine Pretreatment Attenuates Kidney Injury and Oxidative Stress during Orthotopic Autologous Liver Transplantation in Rats. Oxidative medicine and cellular longevity 2016; 2016: 4675817.
40. Liu J, Hu Y, Feng Y, Jiang Y, Guo Y, Liu Y, et al.: BDH2 triggers ROS-induced cell death and autophagy by promoting Nrf2 ubiquitination in gastric cancer. Journal of experimental & clinical cancer research : CR 2020; 39: 123.
41. Klein K, He K, Younes A, Barsoumian H, Chen D, Ozgen T, et al.: Role of Mitochondria in Cancer Immune Evasion and Potential Therapeutic Approaches. Frontiers in immunology 2020; 11: 573326.
42. Holland O, Cuffe J, Dekker Nitert M, Callaway L, Kwan Cheung K, Radenkovic F, et al.: Placental mitochondrial adaptations in preeclampsia associated with progression to term delivery. Cell death & disease 2018; 9: 1150.
43. Huang J, Gao L, Li B, Liu C, Hong S, Min J, et al.: Knockdown of Hypoxia-Inducible Factor 1α (HIF-1α) Promotes Autophagy and Inhibits Phosphatidylinositol 3-Kinase (PI3K)/AKT/Mammalian Target of Rapamycin (mTOR) Signaling Pathway in Ovarian Cancer Cells. Medical science monitor : international medical journal of experimental and clinical research 2019; 25: 4250-4263.

44. Zhao C, Wang M, Cheng A, Yang Q, Wu Y, Jia R, et al.: Duck Plague Virus Promotes DEF Cell Apoptosis by Activating Caspases, Increasing Intracellular ROS Levels and Inducing Cell Cycle S-Phase Arrest. Viruses 2019; 11.
45. Chen J, Leong P, Leung H, Chan W, Li Z, Qiu J, et al.: A Chinese Herbal Formulation, Xiao-Er-An-Shen Decoction, Attenuates Tourette Syndrome, Possibly by Reversing Abnormal Changes in Neurotransmitter Levels and Enhancing Antioxidant Status in Mouse Brain. Frontiers in pharmacology 2019; 10: 812.
46. Varet H, Shaulov Y, Sismeiro O, Trebicz-Geffen M, Legendre R, Coppée J, et al.: Enteric bacteria boost defences against oxidative stress in Entamoeba histolytica. Scientific reports 2018; 8: 9042.
47. Suh K, Chon S, and Choi E: Luteolin alleviates methylglyoxal-induced cytotoxicity in osteoblastic MC3T3-E1 cells. Cytotechnology 2016; 68: 2539-2552.
48. Krejcir R, Krcova L, Zatloukalova P, Briza T, Coates P, Sterba M, et al.: A Cyclic Pentamethinium Salt Induces Cancer Cell Cytotoxicity through Mitochondrial Disintegration and Metabolic Collapse. International journal of molecular sciences 2019; 20.
49. Vangapandu H, Havranek O, Ayres M, Kaipparettu B, Balakrishnan K, Wierda W, et al.: B-cell Receptor Signaling Regulates Metabolism in Chronic Lymphocytic Leukemia. Molecular cancer research : MCR 2017; 15: 1692-1703.
50. Lis P, Dyląg M, Niedźwiecka K, Ko Y, Pedersen P, Goffeau A, et al.: The HK2 Dependent "Warburg Effect" and Mitochondrial Oxidative Phosphorylation in Cancer: Targets for Effective Therapy with 3-Bromopyruvate. Molecules (Basel, Switzerland) 2016; 21.
51. Shirakawa M, Fujiwara Y, Sugita Y, Moon J, Takiguchi S, Nakajima K, et al.: Assessment of stanniocalcin-1 as a prognostic marker in human esophageal squamous cell carcinoma. Oncology reports 2012; 27: 940-6.
52. Jin J, Qiu S, Wang P, Liang X, Huang F, Wu H, et al.: Cardamonin inhibits breast cancer growth by repressing HIF-1α-dependent metabolic reprogramming. Journal of experimental & clinical cancer research : CR 2019; 38: 377.
53. Feng Y, Xiong Y, Qiao T, Li X, Jia L, and Han Y: Lactate dehydrogenase A: A key player in carcinogenesis and potential target in cancer therapy. Cancer medicine 2018; 7: 6124-6136.
54. Chen S, Xu H, Hu F, and Wang T: in vitroIdentification of Key Players Involved in CoCl Hypoxia Induced Pulmonary Artery Hypertension. Frontiers in genetics 2020; 11: 232.
55. Wang X, Hu Z, Wang Z, Cui Y, and Cui X: Angiopoietin-like protein 2 is an important facilitator of tumor proliferation, metastasis, angiogenesis and glycolysis in osteosarcoma. American journal of translational research 2019; 11: 6341-6355.
56. Courtnay R, Ngo D, Malik N, Ververis K, Tortorella S, and Karagiannis T: Cancer metabolism and the Warburg effect: the role of HIF-1 and PI3K. Molecular biology reports 2015; 42: 841-51.
57. Gao H, Liang D, Li C, Xu G, Jiang M, Li H, et al.: 2-Deoxy-Rh2: A novel ginsenoside derivative, as dual-targeting anti-cancer agent via regulating apoptosis and glycolysis. Biomedicine & pharmacotherapy = Biomedecine & pharmacotherapie 2020; 124: 109891.

Figures

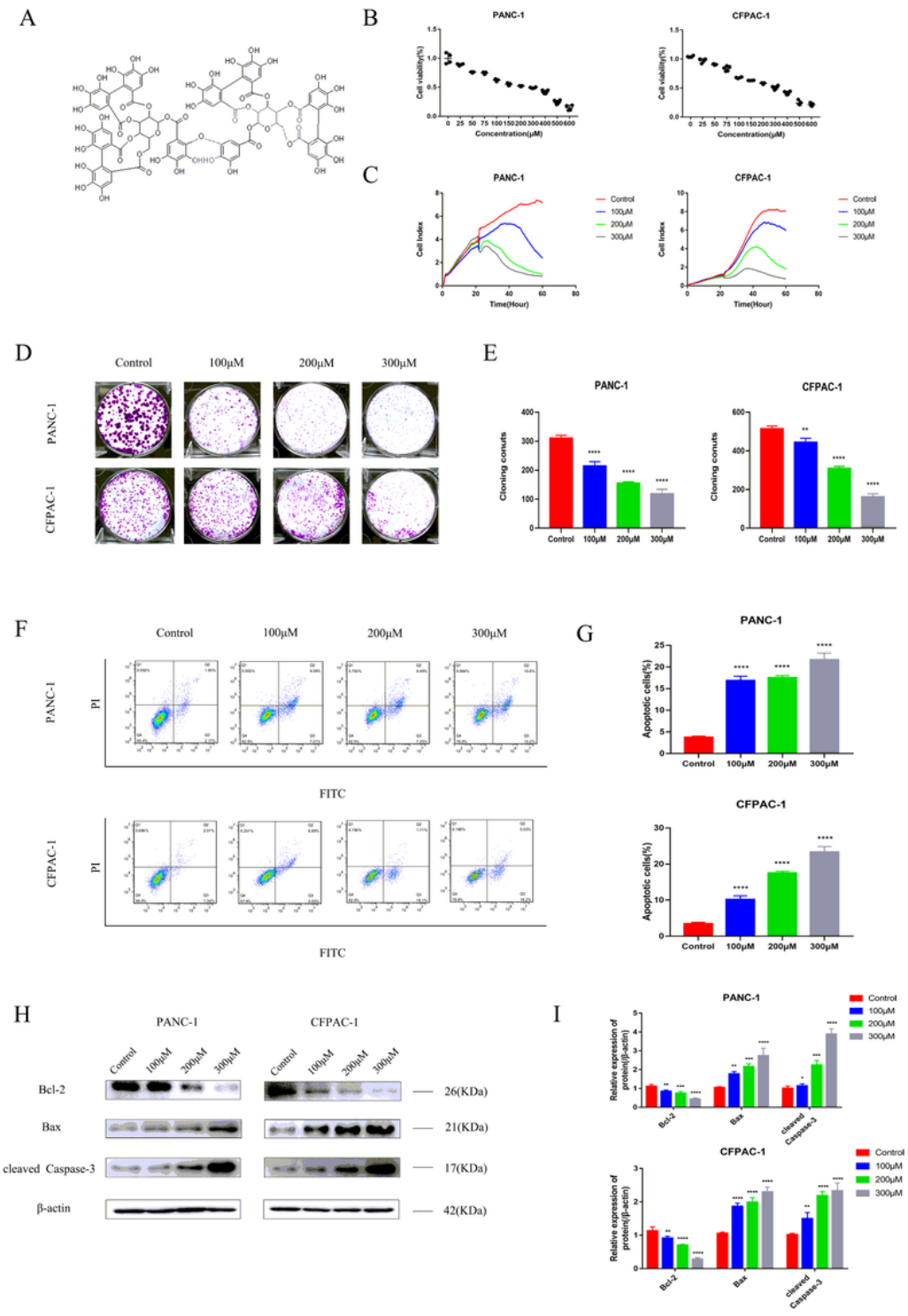

Figure 1

Effect of agrimoniin on PANC-1 and CFPAC-1 cell growth and apoptosis (a) Chemical structure of agrimoniin. (b) CCK8 assay following cells incubated with agrimoniin (25, 50, 75, 100, 150, 200, 300, 400, 500, and 600 μM) or untreated medium for 24 h. (c) RTCA following cancer cells incubated with indicated

concentrations of agrimoniin (100, 200, and 300 μM) or untreated medium for 24 h. (d, e) Colony formation assay following cancer cells incubated with indicated concentrations of agrimoniin (100, 200, and 300 μM) for 24h. (f, g) Cell apoptosis were determined by flow cytometry assay after agrimoniin treatment (0, 100, 200, and 300 μM) for 24 h. (h, i) Western blot assay was used to evaluate the effect of agrimoniin (100, 200, and 300 μM) on apoptosis by detecting apoptosis-related proteins. Results are shown as mean ± SD. * p <0.05, ** p <0.01 *** p <0.001, **** p <0.0001 versus the control group.

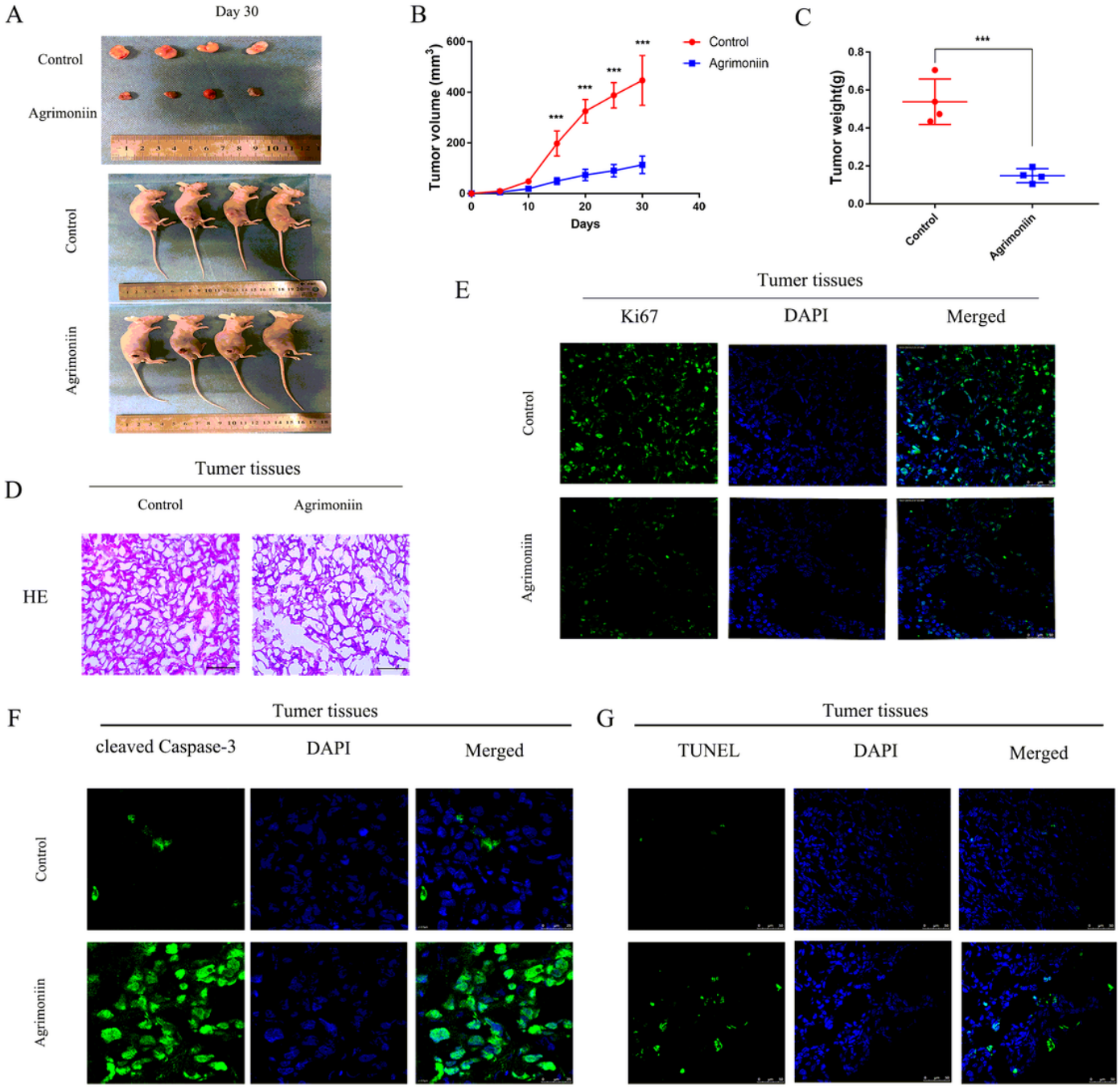

Figure 2

Agrimoniin inhibits the growth of pancreatic cancer cells in vivo (a) The mice were euthanized and the tumors were excised from the mice and photographed after last treatment. (b) The effects of agrimoniin on tumor volumes were measured in xenograft mice. (c) Tumor weights were measured and compared. (d) HE staining was used to evaluate the histological structure of xenograft tumor sections. Bar = 100 μm. (e, f) The expression levels of Ki-67 and cleaved caspase-3 in cancer tissues were detected by immunofluorescence assay. Bar = 50 and 25 μm, respectively. (g) TUNEL staining was used to evaluate the apoptotic cells in the tumor tissue by. Bar = 50 μm. Results are shown as mean ± SD. *** p <0.001, versus the agrimoniin-treated group.

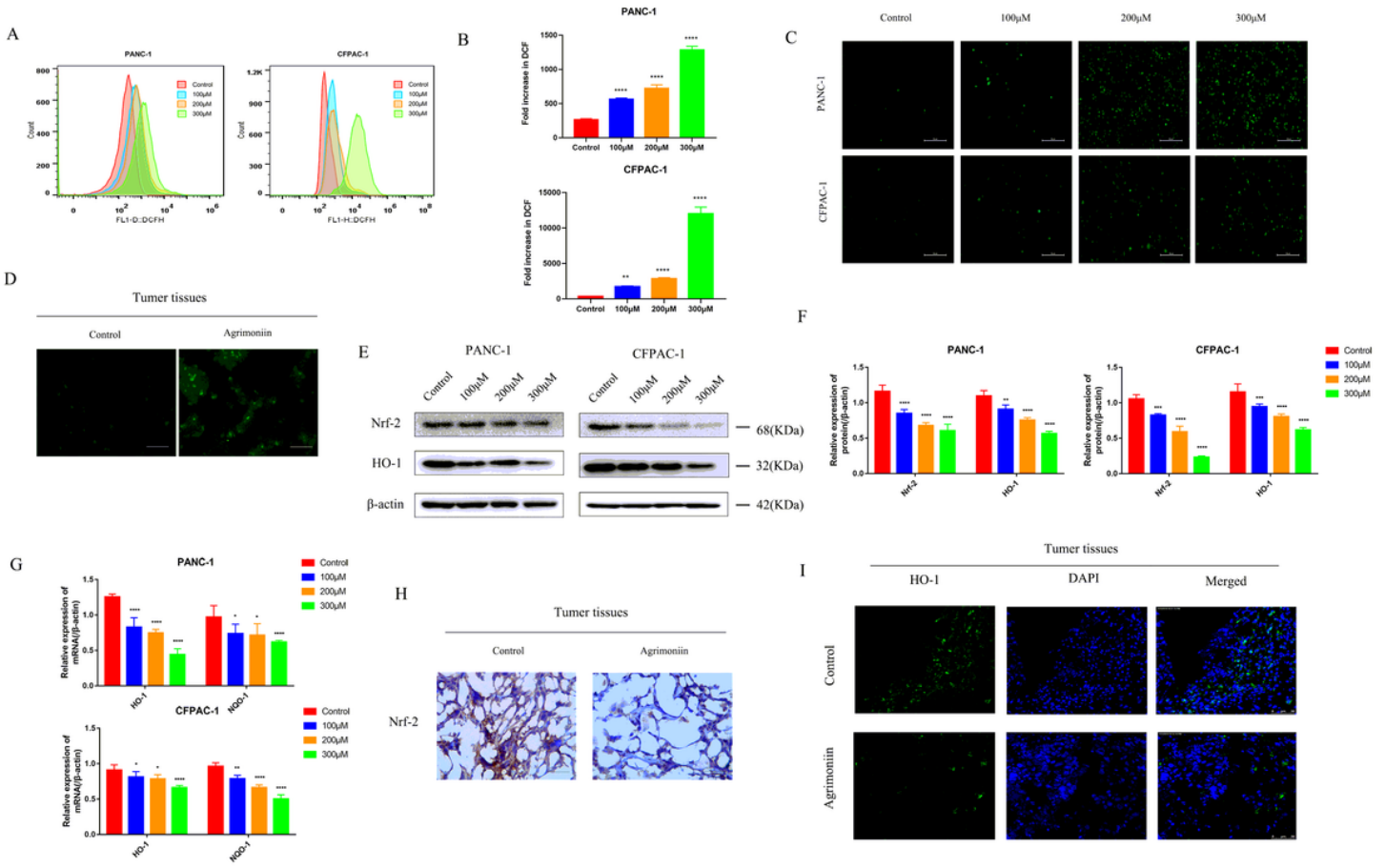

Figure 3

Agrimoniin triggered ROS generation in pancreatic cancer cells (a, b) ROS generation was observed by using flow cytometry following staining with DCFH-DA following agrimoniin treatment (0, 100, 200, and 300 μM) for 24 h. (c) Intracellular ROS generation was measured by using a fluorescence microscope following treatment with agrimoniin for 24 h and staining with DCFH-DA. Bar = 50 μm. (d) Determination of the ROS levels in frozen tissue sections of each group by using a fluorescence microscope. Bar = 50 μm. (e, f) Western blot assay was used to detected the protein expression of Nrf2 and HO-1. (g) Agrimoniin treatment decreased the mRNA expression of NQO1 and HO-1 in cancer cells. (h) Determination of the Nrf2 levels in tissue sections of each group by using a microscope. Bar = 50 μm. (i) The expression levels of HO-1 in cancer tissues were detected by immunofluorescence assay. Bar = 50

μm. Results are shown as mean ± SD. * p <0.05, ** p <0.01 *** p <0.001, **** p <0.0001 versus the control group.

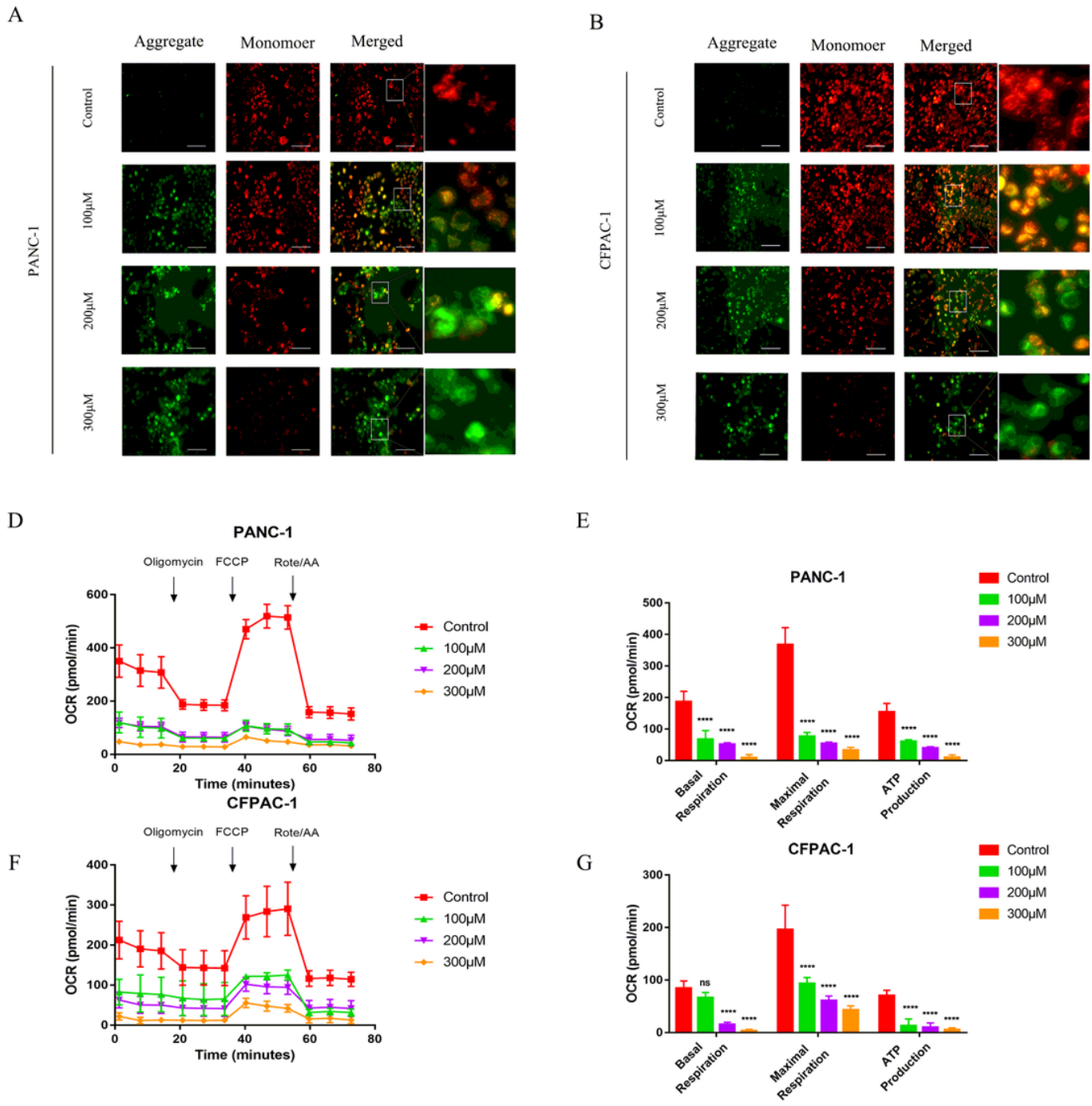

Figure 4

Agrimoniin disrupts mitochondrial function in pancreatic cancer cells (a, b) JC-1 staining assay showed that agrimoniin treated for 24 h decreased the mitochondrial membrane potential in PANC-1 and CFPAC-1 cells. (c, e) Treatment with agrimoniin significantly decreased OCR in cancer cells. (d, f) Basal respiration, maximal respiration, and ATP production of each group was assessed. Results are shown as mean ± SD. **** p <0.0001 versus the control group.

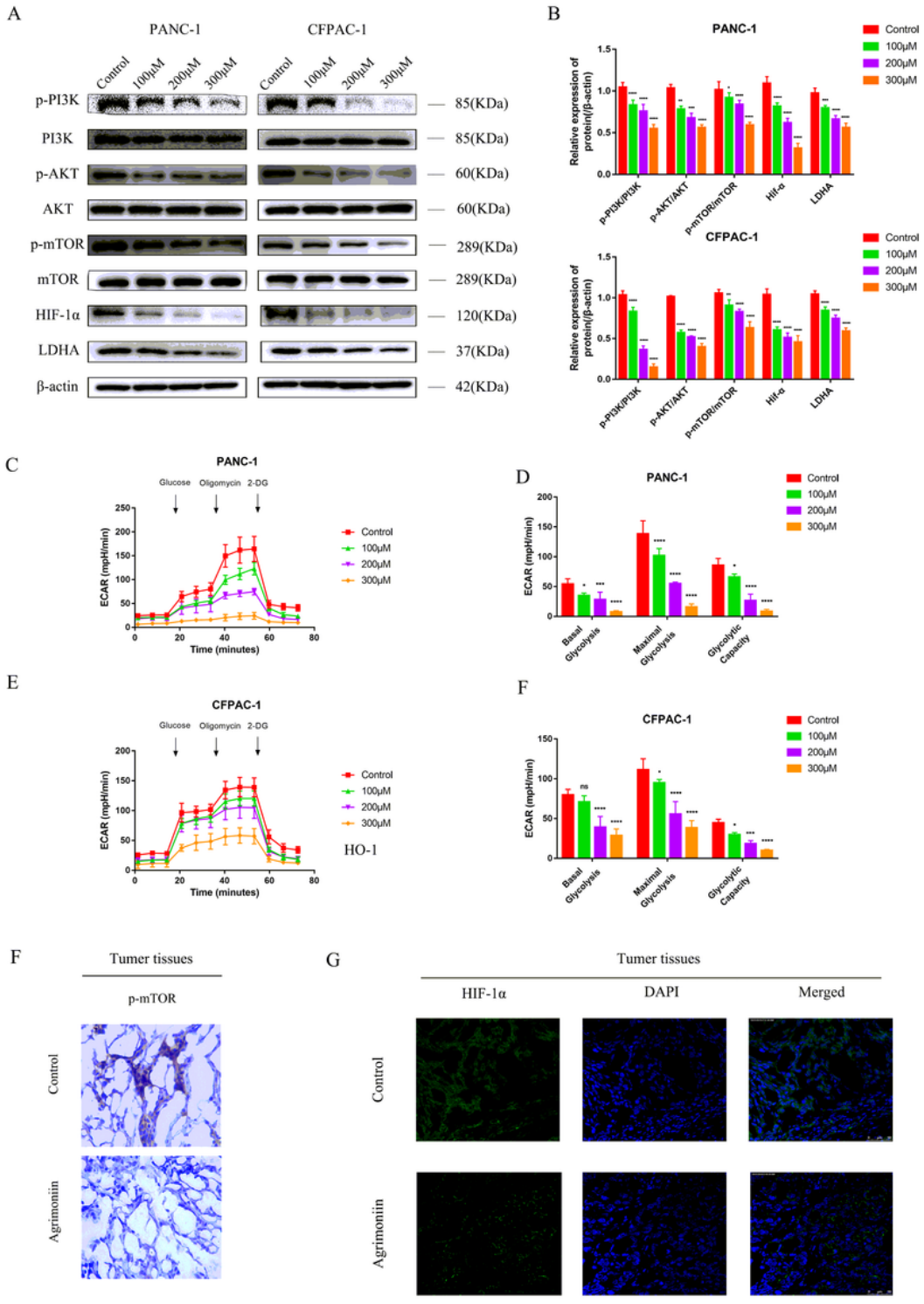

Figure 5

Agrimoniin reduces glycolysis in pancreatic cancer cells. (a, b) Treatment with agrimoniin for 24 h significantly decreased the protein levels of PI3K/AKT/mTOR pathway and the key genes HIF-1α and LDHA. (c, d) Treatment with agrimoniin significantly decreased ECAR in PANC-1 cells and detected in the basal glycolysis, maximal glycolysis, and glycolytic capacity. (e, f) Treatment with agrimoniin significantly decreased ECAR in CFPAC-1 cells and assessed basal glycolysis, maximal glycolysis, and

glycolytic capacity. (g) The expression levels of p-mTOR in cancer tissues were assessed by immunohistochemical staining. Bar = 50 μm. (h) The expression levels of HIF-1α in tissue sections were detected by immunofluorescence assay. Bar = 50 μm. Results are shown as mean ± SD. * p <0.05, ** p <0.01 *** p <0.001, **** p <0.0001 versus the control group.

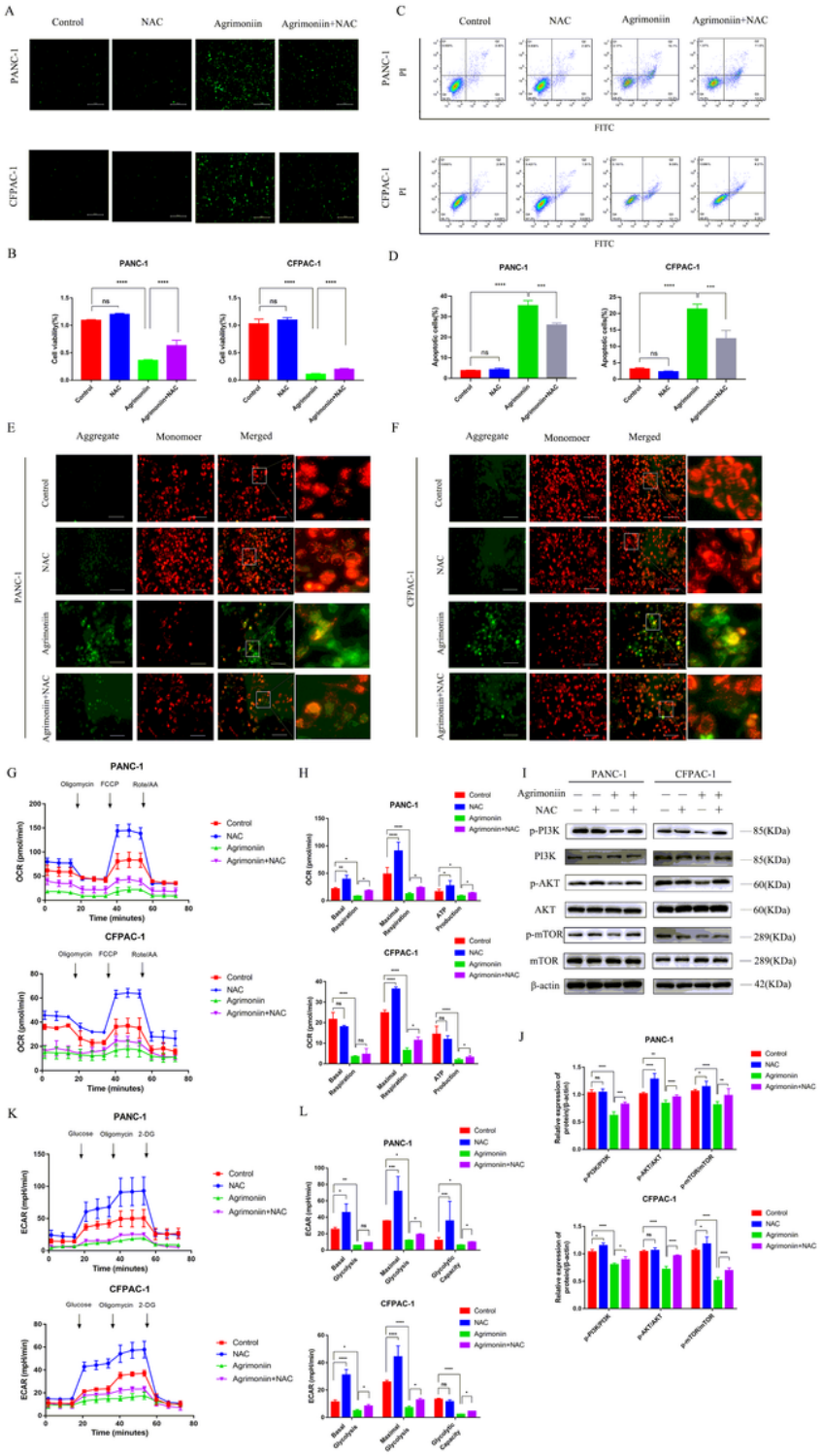

Figure 6

ROS plays an essential role in agrimoniin-induced cell apoptosis. (a) Intracellular ROS generation was measured by using fluorescence microscope following pretreatment with or without NAC in agrimoniin-treated cancer cells and stained with the DCFH-DA probe. Bar = 50 μm. (b) CCK-8 assays was used to evaluate the cell viability with or without NAC treatment in agrimoniin-treated cancer cells. (c, d) Flow cytometry analysis was used to show cell apoptosis in agrimoniin-treated cancer cells with or without NAC. (e, f) After agrimoniin was incubated in cancer cells with or without NAC, ΔΨm was detected by JC-1 staining and detected under a fluorescence microscope. (g) The cells incubated with agrimoniin reversed the change of OCR by NAC. (h) Similar basal respiration, maximal respiration, and ATP production results were obtained. (i, j) Western blot analysis showing the reversed expression of p-PI3K, p-AKT, and p-mTOR in agrimoniin-treated cancer cells after pretreatment with NAC. (k, l) The change of ECAR and basal glycolysis, maximal glycolysis, and glycolytic capacity in agrimoniin-treated pancreatic cancer cells were reversed by pretreatment with NAC. Results are shown as mean ± SD. * $p < 0.05$, ** $p < 0.01$ *** $p < 0.001$, **** $p < 0.0001$.

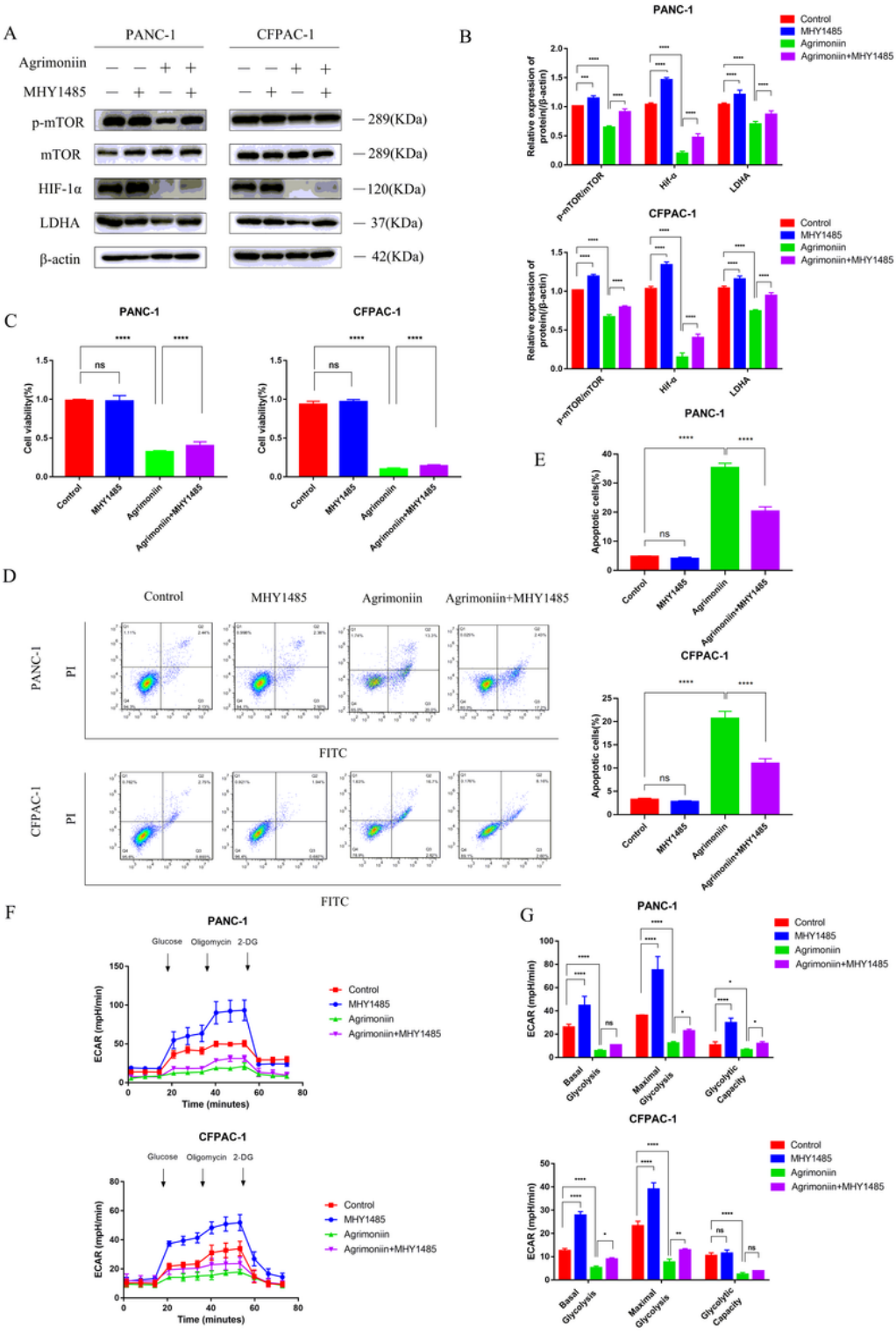

Figure 7

Restoring the mTOR/HIF-1α pathway abolishes the effect of agrimoniin on glycolysis in cancer cells (a, b) The protein levels of mTOR/HIF-1α pathway were analyzed by Western blot analysis during MHY148 pretreatment in agrimoniin-treated cancer cells. (c) CCK-8 assays was used to evaluate the cell viability with or without MHY148 pretreatment in agrimoniin-treated cancer cells. (d, e) Flow cytometry analysis was used to show cell apoptosis in agrimoniin-treated cancer cells with or without MHY148. (f) The

change of ECAR was detected. (g) The changes in basal glycolysis, maximal glycolysis, and glycolytic capacity were measured. Results are shown as mean ± SD. * p <0.05, ** p <0.01 *** p <0.001, **** p <0.0001.

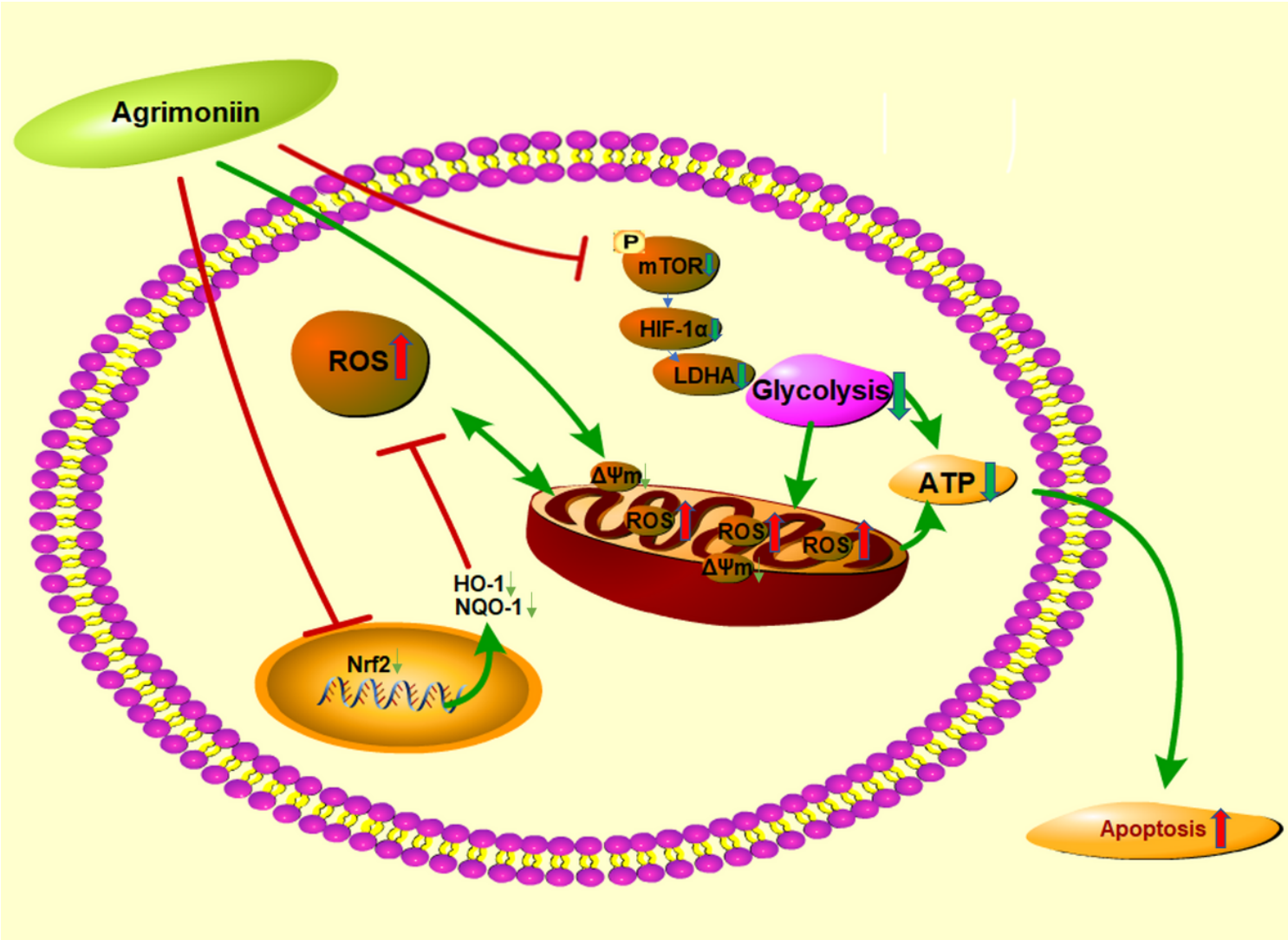

Figure 8

Schematic representation of possible molecular mechanism by which agrimoniin mediated energy metabolism dysfunction and inhibits promotes cell apoptosis in pancreatic cancer cells.